



Methanation of CO₂ over alkali-promoted Ru/TiO₂ catalysts: II. Effect of alkali additives on the reaction pathway

Paraskevi Panagiotopoulou

School of Environmental Engineering, Technical University of Crete, GR-73100, Chania, Greece



ARTICLE INFO

Keywords:
CO₂ methanation
Ru/TiO₂
Alkali promotion
Reaction pathway
DRIFTS

ABSTRACT

The effect of alkali (Li, Na, K, Cs) promotion of TiO₂ on the CO₂ hydrogenation pathway has been investigated over 0.5%Ru/TiO₂ and 5%Ru/TiO₂ catalysts, employing *in situ* FTIR spectroscopy (DRIFTS) and transient-mass spectrometry techniques. In the case of 0.5%Ru/TiO₂ catalysts, characterized by well-dispersed Ru particles, specific activity and selectivity toward methane increases significantly with the addition of suitable amount of alkalis. The nature and population of Ru-bonded carbonyl species, formed on the surface of 0.5%Ru/TiO₂ catalyst under CO₂ hydrogenation conditions, varies significantly upon alkali promotion. The population of reactive Ru_x-CO species, which has been previously found to be direct methane precursors, increases in the presence of alkalis following a trend similar to that of specific activity. Results of DRIFT and mass spectrometry experiments provide evidences that alkali promotion enhances the dissociative adsorption of CO and hydrogenation of the so formed surface carbon to methane, which seems not to be operable over the un-promoted 0.5%Ru/TiO₂ catalyst. In the case of 5%Ru/TiO₂ catalysts, characterized by large Ru particles, both CO₂ methanation activity and the nature/population of intermediate surface species seems not to be significantly affected by the presence of sodium. It is suggested that the structure sensitivity of the reaction predominates to the effect of alkali promotion and therefore, CO₂ methanation activity cannot be further improved.

1. Introduction

Hydrogenation of CO₂ to CH₄ using sustainable H₂ is a promising technology for the elimination of CO₂ in the atmosphere, due to certain advantages offered by the produced methane. In particular, CH₄ can be readily fed into the existing natural gas infrastructure and/or used as energy carrier in power plants [1–5]. Thus, efforts have been made during the last decades in order to develop active and stable catalysts for the production of CH₄ from CO₂ [6–8].

Catalytic performance of dispersed metal catalysts for the CO₂ methanation reaction has been found to depend strongly on the nature of both the metallic phase and the support. Among the various metal-support combinations investigated so far, Ni, Ru and Rh catalysts supported on Al₂O₃ or TiO₂ have been reported to exhibit high activity and methane selectivity at low reaction temperatures [2,5,7–12]. An improvement of catalytic activity and selectivity can be achieved via catalyst doping with various additives, such as alkali (Na, K, Li, Cs) [13–16], alkaline earths (Ca, Ba, Sr, Mg) [14,15,17–19], lanthanides (La, Ce) [14] as well as transition metals (Ni, Co, Zr, W) [14,17,20].

In our recent work, it has been found that CO₂ methanation activity of well-dispersed Ru/TiO₂ catalysts can be enhanced significantly by addition of small amounts of alkalis (Li, Na, K, Cs) on TiO₂ support

[16]. Specific activity was found to go through a maximum with increasing sodium content from 0.0 to 0.4 wt.%, with the sample containing 0.2 wt.% Na exhibiting optimum catalytic activity and methane selectivity. The improvement of catalytic activity upon sodium addition is significantly lower in the case of 5%Ru/TiO₂ catalysts, which is characterized by larger Ru crystallite size. Turnover frequency of 0.5% Ru/0.2%Na-TiO₂ catalyst was found to be higher than that measured over 5%Ru/TiO₂, indicating that small amounts of alkalis can replace part of precious metals, reducing the cost and increasing the efficiency of the CO₂ methanation process.

The investigation of the mechanism of CO₂ methanation reaction has been the subject of several studies. In general, two pathways have been proposed, depending on the nature of the metallic phase and the support employed. According to the first pathway, CO₂ is dissociated on the catalyst surface toward adsorbed CO and oxygen species, which further interact with adsorbed hydrogen atoms leading to CH₄ production [3,21–24]. The second pathway occurs through intermediate production of formate species via the reverse water-gas shift (RWGS) reaction, which results in the formation of adsorbed carbonyl species [25–32]. This species either is dissociated followed by hydrogenation of surface carbon toward methane [21,22,32–35] or is involved in an associative scheme, which leads to methane production through the

E-mail address: ppanagiotopoulou@isc.tuc.gr.

formation of an oxygen-containing carbonyl species [22,26,36–38]. However, depending on the catalyst and the operating conditions employed, part of the adsorbed carbonyl species is desorbed in the gas phase yielding CO and resulting in low CH₄ selectivities [21,27].

It should be noted that, according to the first pathway, formate species, even if produced, is a side product mainly associated with the support. On the other hand, the RWGS reaction is the initial step of the second proposed pathway, and therefore, formate species is the precursor of adsorbed carbonyls. The first mechanistic scheme has been mostly proposed to be operable over supported Rh catalysts, whereas the second scheme is more common over supported Ru catalysts. This agrees well with our previous detailed mechanistic studies over Ru/TiO₂ catalysts, where it was found that the reaction proceeds via the RWGS reaction through the associative CO hydrogenation pathway [26,36].

In the present study, the effect of alkali promotion of 0.5%Ru/TiO₂ and 5%Ru/TiO₂ catalysts on the CO₂ methanation pathway is investigated with respect to promoter type (Li, Na, K, Cs) and loading (0.0–0.40 wt.% Na), employing *in situ* FTIR and mass spectrometry (transient-MS) techniques. The objective is to identify the nature of active sites and surface species which drives selectivity of CO₂ methanation reaction upon alkali addition on TiO₂ support.

2. Experimental

2.1. Catalyst preparation and characterization

Alkali-promoted TiO₂ supports were prepared by impregnation of titanium dioxide powder (Aeroxide P25) with an aqueous solution containing the appropriate amount of Li₂CO₃, NaNO₃, KNO₃ or CsNO₃, following the procedure described elsewhere [16]. Dispersed Ru catalysts were prepared employing the wet impregnation method with the use of the above alkali-promoted TiO₂ powders as supports and Ru(NO)₃₃ (Alfa) as metal precursor salt [16]. The nominal Ru loadings of the catalysts thus prepared were 0.5 and 5 wt%. Catalysts were characterized with respect to their specific surface area (BET), phase composition and crystallite size of TiO₂, ruthenium dispersion and crystallite size employing N₂ physical adsorption (77 K), X-ray diffraction (XRD), selective chemisorption of CO and Transmission Electron Microscopy (TEM), respectively. Results obtained from catalysts characterization can be found in our previous publication [16].

2.2. Kinetic measurements

Catalytic activity of Ru/TiO₂ catalysts for the CO₂ methanation reaction was investigated using an apparatus and following the procedures described in detail elsewhere [16]. Experiments were performed using 100 mg of catalyst, a total flow rate of 150 cm³ min⁻¹ and a feed stream consisting of 5%CO₂ + 20%H₂ (balance He). Results of kinetic measurements and Ru dispersion were used to determine the turnover frequencies (TOFs) of CO₂ consumption, defined as moles of CO₂ converted per surface ruthenium atom per second (see ref [16] for details).

2.3. *In situ* FTIR spectroscopy

The interaction of CO₂/H₂ mixture with the catalyst surface was investigated employing *in situ* Fourier transform infrared (FTIR) spectroscopy. Experiments were carried out using a Nicolet 6700 FTIR spectrometer equipped with a diffuse reflectance (DRIFT) cell (Spectra Tech), an MCT detector and a KBr beam splitter. The gas mixture used in these experiments was consisted of 1%CO₂ + 4%H₂ (in He) and the total flow rate through the DRIFT cell was 30 cm³ min⁻¹. Details on the apparatus and procedures used can be found elsewhere [9].

2.4. Temperature-programmed surface reaction (TPSR) experiments

Temperature-programmed surface reaction (TPSR) experiments were carried out using an Omnistar/Pfeiffer Vacuum mass spectrometer (MS) for on-line monitoring of effluent gas composition. The apparatus and procedures used have been described in detail elsewhere [36]. Briefly, an amount of 150 mg of catalyst was placed in a quartz microreactor and reduced *in situ* at 300 °C for 30 min under flowing hydrogen. The sample was then heated at 500 °C under He flow for 15 min in order to remove adsorbed species from the catalyst surface and subsequently cooled down to room temperature. The flow was then switched to the reaction mixture, consisting of 1%CO₂ + 4% H₂ (in He), for 15 min at RT, followed by linear heating ($\beta = 30^\circ\text{C min}^{-1}$) at 740 °C. The total flow rate through the reactor was 30 cm³ min⁻¹.

3. Results and discussion

3.1. Effect of alkali additives on catalytic activity of 0.5% and 5%Ru/TiO₂ catalysts

In our recent study over Ru/TiO₂ catalysts it was found that the addition of small amounts of alkalis (Li, Na, K, Cs) on TiO₂ support does not affect significantly both ruthenium dispersion and mean crystallite size [16]. However, specific activity for the CO₂ methanation reaction can be significantly enhanced in a manner which depends strongly on dispersed Ru loading (or Ru crystallite size) as well as the nature and loading of the promoter. Briefly, in the case of 0.5%Ru/TiO₂ catalysts, which are characterized by small Ru particles (1.8–2.8 nm) [16], both the intrinsic reaction rate and methane selectivity follows the order of TiO₂ (unpromoted) < Li ~ K < Cs < Na, with the Na-promoted sample being around 3 times more active compared to the unpromoted catalyst. In addition to methane, carbon monoxide is also produced, the selectivity of which presents the opposite order with respect to alkali type. Turnover frequency (TOF) of CO₂ conversion exhibits a volcano-type dependence on the sodium content, with the sample containing 0.2 wt.% Na exhibiting optimum catalytic activity (Fig. 1A). The same trend is observed for methane selectivity, which increases from 87 to 98% with increasing Na loading from 0 to 0.2 wt.%, whereas CO selectivity presents the opposite behavior (Fig. 1B). As it can be seen in Fig. 1A, the effect of alkali promotion is less pronounced in the case of 5%Ru/TiO₂ catalysts, which are characterized by larger Ru particles (3.7–4.9 nm) [16]. Specific activity increases only slightly (by a factor of 1.4) upon sodium addition on TiO₂. This is also the case for methane selectivity, which is almost 100% for all the (promoted or not) 5%Ru/TiO₂ catalysts investigated, whereas only traces of CO are detected (Fig. 1B). Evidence has been provided that addition of alkalis promotes hydrogenation of intermediate produced CO to CH₄ over well dispersed Ru particles, whereas large Ru particles do not “feel” the presence of the promoter.

3.2. Mechanistic aspects of CO₂ methanation reaction over alkali promoted Ru/TiO₂ catalysts

3.2.1. 0.5% Ru/TiO₂ catalysts

3.2.1.1. *In situ* FTIR spectra. The CO₂ methanation reaction has been investigated with the use of FTIR spectroscopy technique in an attempt to identify the nature of active sites and adsorbed species, which are responsible for the increased catalytic activity with alkali addition. It should be noted that, FTIR results of the present study cannot be used to extract kinetic information, but only qualitative information related to the nature and variation of the relative population of adsorbed surface species with reaction temperature and catalyst employed.

The *in situ* DRIFT spectra obtained following exposure of the pre-reduced unpromoted 0.5%Ru/TiO₂ catalyst to a flowing 1%CO₂ + 4% H₂ (in He) mixture at 25 °C for 15 min and subsequent stepwise heating at 450 °C are shown in Fig. 2A. The spectra obtained at temperatures

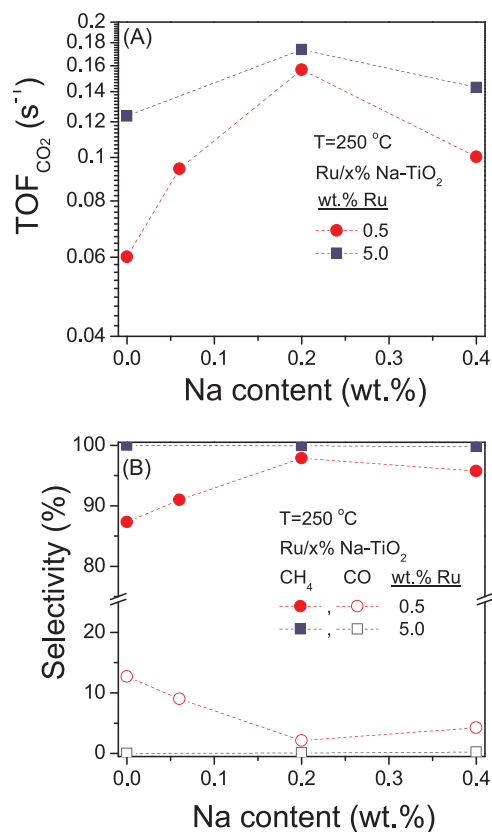


Fig. 1. Effect of sodium loading (wt.%) on the (A) turnover frequencies of CO₂ conversion and (B) selectivity toward CH₄ and CO obtained at 250 °C over 0.5% Ru and 5%Ru/TiO₂ catalysts. Experimental conditions: Mass of catalyst: 100 mg; particle diameter: 0.18 < d_p < 0.25 mm; Feed composition: 5%CO, 20% H₂ (balance He); Total flow rate: 150 cm³ min⁻¹.

lower than 100 °C are characterized only by bands located below 1700 cm⁻¹ (trace a) which, can be attributed to formate (bands at ca. 1553, 1382 and 1318 cm⁻¹) and bicarbonate (bands at ca. 1646 and 1426 cm⁻¹) species associated with the support [25,36,39–41]. Increasing temperature at 150 °C (trace c) results in the development of bands in the $\nu(\text{CO})$ region, which have been previously assigned to multicarbonyl species adsorbed on partially oxidized Ruⁿ⁺ sites (Ruⁿ⁺(CO)_x, band at 2060 cm⁻¹) [26,27,36,42], CO species linearly-bonded on reduced Ru sites (Ru_x-CO, band at 2020 cm⁻¹) [26,27,32,36,42,43] and terminal CO species adsorbed on Ru sites located at the metal-support interface ((TiO₂)Ru-CO, band at 1967 cm⁻¹) [26,27,36,44].

Increasing temperature up to 250 °C results in an increase of the band due to $\text{Ru}_x\text{-CO}$ species, followed by a decrease of the relative intensity of the band due to $(\text{Ru}^{n+}(\text{CO})_x)$ species, which disappears from the catalyst surface upon heating at temperatures higher than 300 °C. This has been previously attributed to interconversion of $\text{Ru}^{n+}(\text{CO})_x$ species to $\text{Ru}_x\text{-CO}$ species most probably due to H_2 -induced reductive agglomeration of Ru^{n+} sites to Ru_x [27,36]. The 2020 cm^{-1} band shifts toward lower wavenumbers with increasing temperature [26,45] and is the only band observed in the $\nu(\text{CO})$ region at temperatures higher than 300 °C (trace f). The red shift of $\text{Ru}_x\text{-CO}$ band has been previously assigned to the decrease of the dipole-dipole coupling with decreasing coverage [45]. The decrease of the intensity of the latter band above 300 °C is accompanied by the appearance of a new weak band at 3015 cm^{-1} assigned to gas-phase CH_4 [26], indicating (a) the onset of CO_2 methanation reaction and (b) that $\text{Ru}_x\text{-CO}$ species is active for the title reaction. Regarding the $(\text{TiO}_2)\text{Ru}\text{-CO}$ species, its relative population is eliminated from the catalyst surface at temperatures lower than 250 °C, implying that this species is either desorbed producing gas phase CO or diffuses to the crystallite surface, as evidenced by the increased relative intensity of band due to $\text{Ru}_x\text{-CO}$.

In our previous studies over Ru/TiO₂ catalysts, it has been found that, in the absence of H₂ in the feed, CO₂ is mainly adsorbed on the support surface [46], leading only to the development of bands due to carbonate species associated with TiO₂ support [26,36]. This provides evidence that CO₂ dissociation does not take place under the present

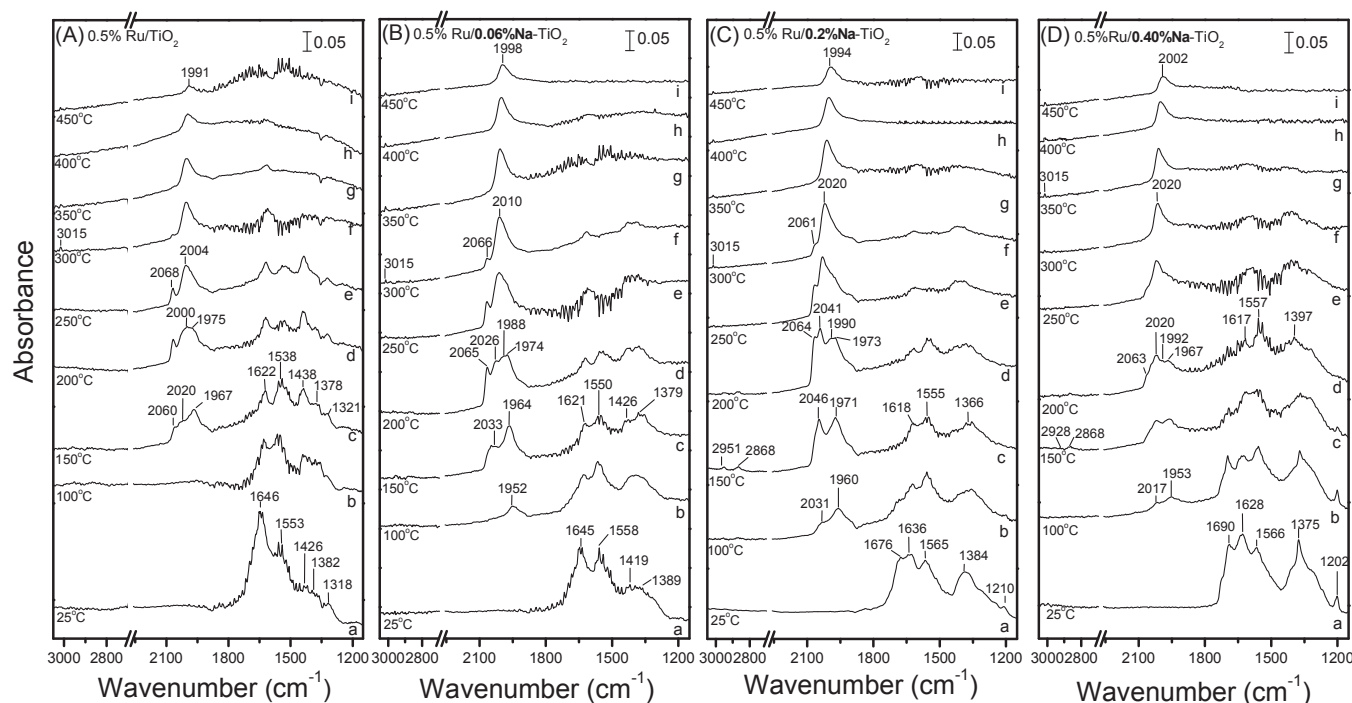


Fig. 2. DRIFT spectra obtained over sodium-promoted 0.5%Ru/TiO₂ catalysts of variable sodium loadings (wt.%) following interaction with 1%CO₂ + 4%H₂ (in He) at 25 °C for 15 min and subsequent stepwise heating at 450 °C under the same flow.

experimental conditions in agreement with literature over Pd/Al₂O₃ [30] and Ru/Al₂O₃ [29] catalysts. Hydrogen addition in the gas stream facilitates the conversion of CO₂ to CO resulting in the formation of Ru-bonded carbonyl species on the catalyst surface (Fig. 2A). It is of interest to note that the relative population of formate species associated with the support starts decreasing at temperatures higher than 150 °C (trace c), where Ru-bonded carbonyl species start to be developed. This provides evidence that CO₂ methanation proceeds through intermediate production of formates via the RWGS reaction. According to this scheme hydrogen adsorbed on Ru surface is diffused at the metal-support interface where it reacts with CO₂, which is mainly adsorbed on TiO₂, yielding formates and, eventually, adsorbed CO species [25–30]. It has been proposed that part of Ru-bonded carbonyl species interacts with adsorbed hydrogen atoms to form methane in the gas phase, whereas the rest is possibly desorbed yielding CO in the gas phase [27]. Taking into account that the spectra obtained above 250 °C, where CO₂ methanation reaction initiates, is dominated by the band attributed to Ru_x-CO, it can be suggested that CO species linearly-adsorbed on reduced Ru sites are direct precursors of methane in agreement with previous studies [9,26,42,47–49].

Regarding the methanation mechanism of the intermediate produced CO, it has been proposed to occur via either a dissociative or an associative pathway. According to the former pathway, CO is dissociatively adsorbed on Ru surface followed by hydrogenation of surface carbon toward methane [21,22,32–34]. As it will be discussed below, the occurrence of the dissociative CO adsorption can be confirmed by a number of indications in the DRIFTS spectra obtained under CO₂/H₂ conditions (e.g., intermediate formation of CH_{x,ad} species originating from hydrogenation of surface carbon, creation of oxidized Ru sites), which are not provided in the results of Fig. 2A. According to the associative pathway, which is enhanced over Ru catalysts, it has been proposed to involve the formation of an oxygen-containing intermediate species and, eventually, methane in the gas phase [22,26,36–38]. Although, no direct evidence for the existence of such intermediate was obtained in the present study, it is possible that a similar associative pathway is operable for the hydrogenation of Ru_x-CO species (Fig. 1A).

In Fig. 2B are shown the in situ DRIFT spectra obtained from 0.5%Ru/0.06%Na-TiO₂ catalyst under CO₂ hydrogenation conditions. The spectrum recorded at 25 °C (trace a) is characterized only by bands (1645, 1558, 1419 and 1389 cm⁻¹) assigned to formate/carbonate species associated with the support. Ruthenium-bonded carbonyl species (band at 1952 cm⁻¹) starts to be developed at 100 °C (trace b), i.e. at lower temperatures compared to the unpromoted sample. This indicates that interaction of H₂ with CO₂ to yield Ru-CO species is enhanced over sodium-promoted catalyst. Increase of temperature at 150 °C (trace c) results in the development of a well resolved band at 1964 cm⁻¹, which can be attributed to (TiO₂)Ru-CO, and a broad feature centered at ca. 2033 cm⁻¹. The broadness of the latter band indicates that it consists of more than one overlapping peaks.

Further increase of temperature at 200 °C under 1%CO₂ + 4%H₂ flow results in an increase of the intensities of bands in the ν(CO) region, and in the development of well-resolved peaks located at 2065, 2026, 1987 and 1974 cm⁻¹ (trace d). The peak at 2065 cm⁻¹ is due to multicarbonyl species adsorbed on partially oxidized Ru sites (Ruⁿ⁺(CO)_x). Comparison of the spectra presented in Fig. 2A and B shows that the relative population of Ruⁿ⁺(CO)_x species is higher in the case of 0.5%Ru/0.06%Na-TiO₂ catalyst. Partially oxidized Ruⁿ⁺ sites can be formed either by dissociative adsorption of CO on reduced Ru sites and/or by oxidative disruption of small Ru clusters with the participation of hydroxyl groups of the support [27,43,50]. The latter pathway is enhanced over well-dispersed Ru catalysts [27,42], which is the case for both 0.5%Ru/TiO₂ and 0.5%Ru/0.06%Na-TiO₂ samples. However, Ru crystallite size is not affected upon sodium addition, taking values of 2.1–2.2 nm [16]. This indicates that the observed increase of the relative intensity of Ruⁿ⁺(CO)_x band over the alkali

promoted sample is not related to alterations of Ru crystallite size, and most possibly it is not driven by enhancement of interaction of Ru crystallites with hydroxyl groups of TiO₂.

The band at 2026 cm⁻¹ is characteristic of Ru_x-CO species, whereas that at 1974 cm⁻¹ is attributed to (TiO₂)Ru-CO species. The relative intensity of the former band increases with increasing temperature, whereas the opposite is observed for the latter band. Thus, it can be assumed that an interconversion of (TiO₂)Ru-CO to Ru_x-CO species takes place with increasing temperature. Regarding the band at 1988 cm⁻¹, which is not discernible in the spectra obtained from the unpromoted catalyst, it has been previously attributed to monocarbonyl species adsorbed on partially oxidized ruthenium sites (Ruⁿ⁺-CO) [36,42,44,48]. Interestingly, the simultaneous appearance of Ruⁿ⁺(CO)_x and Ruⁿ⁺-CO species at 200 °C (trace d) implies the formation of partially oxidized ruthenium sites (Ruⁿ⁺) on the catalyst surface. This may take place via the Boudouard reaction, which can be described by the following steps:



It can then be suggested that the formation of Ru-O species during dissociative adsorption of CO (Eq. (2)) corresponds to the Ruⁿ⁺ sites responsible for the adsorption bands at ca 2065 and 1988 cm⁻¹, which appears at temperatures around 200 °C upon sodium addition (Fig. 2B).

Bands due to Ruⁿ⁺(CO)_x and Ruⁿ⁺-CO species disappear at temperatures above 300 °C, indicating that are either thermally not stable or interconverted to Ru_x-CO species most probably due to H₂-induced reductive agglomeration of Ruⁿ⁺ sites to Ru_x. The band due to Ru_x-CO species is the dominant spectral feature at temperatures as high as 450 °C and shifts toward lower vibrational frequencies with increasing temperature (from 2033 cm⁻¹ at 150 °C (trace c) to 1998 cm⁻¹ at 450 °C (trace i)), in agreement with previous studies [36,45].

The development of the weak band due to gas-phase methane (3015 cm⁻¹) at temperatures above 300 °C (trace f) [44,51] implies that hydrogenation of intermediate CO is initiated at temperatures where Ru_x-CO become the dominant surface species. This indicates that, as for the unpromoted sample, monocarbonyl species adsorbed on reduced Ru sites are direct methane precursors in the presence of alkalis.

Qualitatively similar DRIFT spectra were obtained from the most active 0.5%Ru/0.2%Na-TiO₂ catalyst (Fig. 2C). The main differences observed compared to the 0.5%Ru/0.06%Na-TiO₂ sample are: (a) two well-resolved bands located at ca. 1676 and 1210 cm⁻¹ are discernible at 25 °C (trace a), which disappear at temperatures higher than 100 °C. Similar bands, detected on spectra obtained from potassium promoted Ru(001), have been previously assigned to CO₂- anion [52]. It has been proposed that in the presence of alkali metal atoms the work function of the surface decreases, resulting in charge transfer to an empty CO₂ π*-orbital [53]. Thus, the direct formation of CO₂- was suggested, taking place via interaction with a surface alkali atom. Therefore, CO₂- anions may be decomposed toward surface carbonate and carbonyl species according to:



(b) The relative intensity of the band due to Ru_x-CO species (2046 cm⁻¹ at 150 °C, trace c) is significantly higher over the catalyst containing 0.2 wt.% Na, indicating that the formation of Ru_x-CO species is enhanced with increasing sodium content. (c) Two new bands located at 2951 and 2868 cm⁻¹ start to be developed at 150 °C (trace c), which can be assigned to C-H stretching vibrations in methyl groups (CH_{3,ad}) and to asymmetric C-H vibrations in methylene groups (CH_{2,ad}), respectively [26,48,51]. A possible route for the formation of such species is via successive hydrogenation of surface carbon atoms (produced via dissociative adsorption of CO (Eqs. (1)–(3)), by adsorbed hydrogen

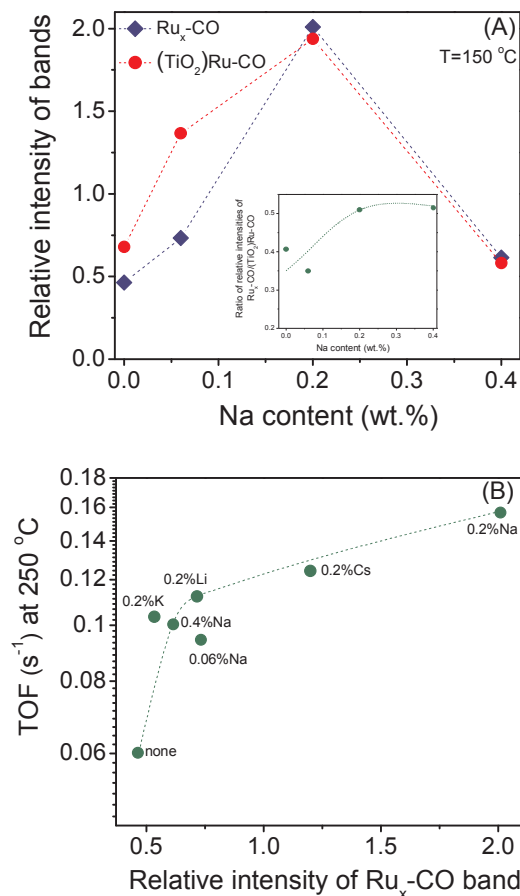


Fig. 3. (A) Relative intensity of bands due to $\text{Ru}_x\text{-CO}$ and $(\text{TiO}_2)\text{Ru-CO}$ at 150°C as a function of Na content. Inset: Effect of Na content on the ratio of relative intensities of $\text{Ru}_x\text{-CO}/(\text{TiO}_2)\text{Ru-CO}$ species. (B) Effect of the relative intensity of band due to $\text{Ru}_x\text{-CO}$ species on the turnover frequencies of CO_2 conversion obtained at 250°C over alkali-promoted 0.5%Ru/TiO₂ catalysts.

atoms, which eventually leads to methane formation. The latter bands disappear above 300°C , where the band due to gas phase methane (3015 cm^{-1}) appears (trace f), indicating that they are active intermediates. Such $\text{CH}_{x,\text{ads}}$ species may be also formed on the surface of the sample containing 0.06 wt. % Na, but their relative population may be smaller and thus, they couldn't be discerned.

DRIFT spectra obtained from the sample containing 0.4 wt. % Na (Fig. 2D) are qualitatively similar, regarding variation of adsorbed species with temperature, with the samples containing 0.06 (Fig. 2B) and 0.2 wt. % Na (Fig. 2C). However, the relative intensity of bands due to $\text{Ru}^{n+}\text{-CO}$ and $\text{Ru}^{n+}\text{(CO)}_x$ species is, generally, lower indicating that the formation of partially oxidized Ru^{n+} sites is suppressed for higher Na loadings. This is also the case for the population of $\text{CH}_{x,\text{ads}}$ species, most possibly due to suppression of dissociative adsorption of CO over this sample. Moreover, it is observed that the relative population of formate/carbonate species adsorbed on the support surface is higher compared to Ru-bonded carbonyl species. This may imply that although CO_2 is converted to formate species via the RWGS reaction, their transformation to reactive carbonyl species is suppressed for high Na content and thus, resulting in lower catalytic activity (Fig. 1A). This can be clearly seen in Fig. 3A, where the relative intensity of bands due to $\text{Ru}_x\text{-CO}$ and $\text{Ru}(\text{TiO}_2)\text{-CO}$ species at 150°C are plotted as a function of Na content. Interestingly, the relative intensity of both bands goes through a maximum for the sample presenting optimum methanation activity (0.5%Ru/0.2%Na-TiO₂) and decreases substantially for the sample containing 0.4 wt. %.

In our previous study it was found that the number of sites located

at the metal-support interface increases with increasing Na or Cs concentration followed by an increase of their adsorption strength toward CO [54–56]. The WGS activity was enhanced over catalysts exhibiting an intermediate CO heat of adsorption and thus, the specific reaction rate goes through a maximum for catalysts with intermediate alkali content [55,57]. In the case of Ru/TiO₂ catalysts, optimum results were observed for the sample containing 0.2 wt. % Na [55], which was also the most active catalyst for the CO_2 methanation reaction in the results of the present study (Fig. 1A). As discussed above, the RWGS reaction is the initial step on the CO_2 hydrogenation pathway, resulting in the conversion of CO_2 toward adsorbed CO species. It can then be suggested that the population and the adsorption strength of the produced carbonyl species increases with increasing Na content from 0 to 0.2 wt. %, favoring CO dissociation and hydrogenation of surface carbon toward CH_4 , rather than desorption of CO in the gas phase. It should be noted that the existence of more than one peaks in the $\nu(\text{CO})$ region makes difficult the determination of peak maxima of bands due to carbonyl species. Therefore, based on DRIFT spectra of Fig. 2, there is no direct evidence related to the adsorption strength of adsorbed CO species. However, as discussed above, clear indications for the occurrence of the Boudouard reaction upon alkali addition are provided, including the formation of carbonyl species adsorbed on partially oxidized Ru^{n+} sites and the formation of $\text{CH}_{x,\text{ads}}$ species. The ability of alkalis to enhance CO dissociation has been also reported by other researchers [58–61]. For example, Kiskinova [59] found that the presence of alkali atoms induces CO decomposition on Ni(100) surface, which is enhanced with increasing alkali concentration due to an increase of the amount of electron charge localized on Ni surface. Similarly, Tomanek et al. [60] found that the activation energy for CO dissociation on Ni(110) surface decreases in the presence of K, due to variations in the population of the CO $2\pi^*$ orbital for a stretched CO molecule. Moreover, potassium was found to favor CO binding strengths on the surface of Fe (100), leading to an increase of CO dissociation ability compared to bare iron surface [58].

Based on the above, it can be suggested that in the presence of sodium the formation of Ru-bonded carbonyl species ($\text{Ru}_x\text{-CO}$, $(\text{TiO}_2)\text{Ru-CO}$) occurs at lower temperatures, with their relative population being higher compared to that of unpromoted sample (Fig. 3A). Increase of temperature may result in a progressive diffusion of $(\text{TiO}_2)\text{Ru-CO}$ species to the crystallite surface leading to an increased population of the reactive $\text{Ru}_x\text{-CO}$ species. This can be seen in the inset of Fig. 3A, where the ratio of relative intensities of $\text{Ru}_x\text{-CO}$ to $(\text{TiO}_2)\text{Ru-CO}$ species (defined as $I_{\text{Ru}_x\text{-CO}}/(I_{\text{Ru}_x\text{-CO}} + I_{(\text{TiO}_2)\text{Ru-CO}})$) is plotted as a function of Na content. It seems that the fraction of CO species linearly-bonded on reduced Ru sites relative to the total amount of surface carbonyl species at 150°C increases significantly with increasing sodium loading from 0 to 0.2 wt. %, suggesting that $\text{Ru}_x\text{-CO}$ are the active species for CO_2 methanation reaction. The $\text{Ru}_x\text{-CO}$ species are then decomposed to surface carbon and Ru-O species, giving rise to the formation of $\text{CH}_{x,\text{ads}}$ as well as $\text{Ru}^{n+}\text{(CO)}_x$ and $\text{Ru}^{n+}\text{-CO}$ species, respectively. The $\text{CH}_{x,\text{ads}}$ species are eventually desorbed as methane in the gas phase, whereas $\text{Ru}^{n+}\text{(CO)}_x$ and $\text{Ru}^{n+}\text{-CO}$ species either yield CO in the gas phase or interconverted to $\text{Ru}_x\text{-CO}$. It is worth noted that although the ratio of $I_{\text{Ru}_x\text{-CO}}/(I_{\text{Ru}_x\text{-CO}} + I_{(\text{TiO}_2)\text{Ru-CO}})$ takes similar values for the samples containing 0.2 and 0.4 wt. % Na, catalytic activity of the latter sample is significantly lower, because as discussed above the population of both monocarbonyl species ($\text{Ru}_x\text{-CO}$, $(\text{TiO}_2)\text{Ru-CO}$) decreases (Fig. 3A).

Qualitatively similar results were obtained from (0.2 wt. %) K-, Li- and Cs-promoted 0.5%Ru/TiO₂ catalysts upon interaction with 1% CO_2 + 4% H_2 (in He) in the temperature range of 25–450 °C (Fig. S1) and, therefore, will not be discussed further. Results imply that a similar reaction pathway is operable for all alkali-promoted 0.5%Ru/TiO₂ catalysts. Correlation of CO_2 methanation activity with the population of $\text{Ru}_x\text{-CO}$ species can be seen in Fig. 3B, where TOF obtained at 250°C is plotted as a function of the relative intensity of the corresponding $\text{Ru}_x\text{-CO}$ band for all alkali-promoted 0.5%Ru/TiO₂ catalysts. Specific

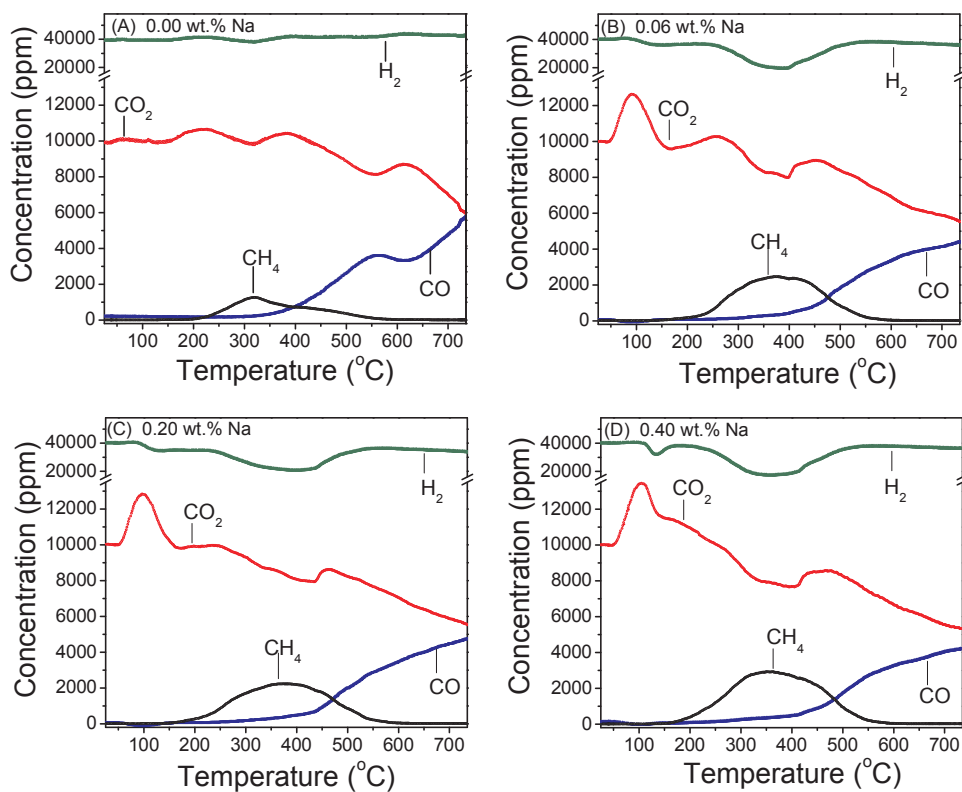


Fig. 4. Transient-MS responses of CO, CO₂, CH₄ and H₂ obtained over sodium-promoted 0.5%Ru/TiO₂ catalysts of variable sodium loadings (wt.%) following interaction with 1%CO₂ + 4%H₂ (in He) at 25 °C for 15 min and subsequent linear heating at 740 °C.

activity progressively increases with the population of CO species linearly-bonded on reduced Ru sites, providing additional evidences that they are active intermediates for the conversion of CO₂ to CH₄. It can then be argued that the increase of the population of the Ru_xCO species upon alkali addition may be responsible for the improvement of CO₂ methanation activity. It should be noted, however, that, apart from CO₂/H₂ ratio (1/4), the experimental conditions (e.g. mass of catalyst, total flow rate, feed composition) used in catalytic performance tests are not identical with those used in DRIFT experiments. Therefore, correlations between Na content and TOFs with the relative intensities of DRIFT bands presented in Fig. 3 can be used only for qualitatively comparison.

3.2.1.2. Transient MS results. The CO₂ hydrogenation reaction over Na-promoted 0.5%Ru/TiO₂ catalysts has also been investigated with the use of transient-MS technique. Fig. 4A presents the concentrations of reactants and products at the reactor effluent as functions of reaction temperature, which have been obtained following interaction of the unpromoted catalyst with 1%CO₂ + 4%H₂ (in He) mixture at 25 °C and subsequent linear heating up to 740 °C.

As it can be seen, the CO₂ methanation reaction initiates at temperatures higher than 200 °C as evidenced by the progressive decrease of both CO₂ and H₂ concentrations as well as by evolution of CH₄ in the gas phase. The methane profile consists of a broad peak exhibiting a maximum at ca 320 °C, which is accompanied by a shoulder at temperatures higher than 400 °C. The concentration of CH₄ is eliminated above ca 600 °C, due to thermodynamic limitations [36]. At temperatures above ca 400 °C the concentration of CO₂ continues to decrease followed by evolution of CO, indicating the occurrence of the RWGS reaction.

Transient-MS results obtained from the Na-promoted 0.5%Ru/TiO₂ catalysts are shown in Fig. 4B, C and D for Na loadings of 0.06, 0.20 and 0.40 wt.%, respectively. Comparison of the results obtained with those discussed above for the unpromoted catalyst shows the following

differences: (a) The total amount of methane produced is significantly higher in the presence of Na, confirming the beneficial effect of alkali addition on CO₂ methanation activity. (b) CO concentration starts increasing at higher temperatures (~ by 50 °C), indicating that CO evolution in the gas phase, at a given temperature, decreases upon alkali promotion. (c) At temperatures lower than 200 °C evolution of CO₂ takes place, resulting in the appearance of a well-resolved peak. This peak, which, only, appears in the presence of alkalis, can be attributed to the Boudouard reaction [36,49,62,63], i.e., the dissociation of the intermediate produced Ru-bonded carbonyls. A small consumption of H₂ observed in Fig. 4B, C and D at slightly higher temperatures than those of CO₂ peak evolution, for the Na-containing samples, can be attributed to hydrogenation of surface carbon formed via CO dissociation. Results of Fig. 4 agree well with DRIFT spectra of Fig. 2, where it was shown that formation of CH_{x,ads} and carbonyl species adsorbed on partially oxidized Ru sites, produced following the dissociative adsorption of CO, takes place in the temperature range of 150–200 °C. The detection of the latter species at slightly higher temperatures (Fig. 2B, C and D) compared to evolution of CO₂ in the gas phase (Fig. 4B, C and D) may be related to the slightly different experimental conditions (e.g. mass of catalyst, reactor type) used in MS experiments compared to DRIFT experiments. The absence of CO₂ peak in the MS profile of the unpromoted catalyst provides evidence that the Boudouard reaction is strongly enhanced in the presence of alkalis.

Comparison of results presented in Fig. 4 with catalytic performance results conducted under steady state conditions [16] shows that, in the latter case, optimum CO₂ conversion to CH₄ was achieved at around 450 °C, whereas CH₄ peak in transient-MS experiments exhibited a maximum at around 350 °C for all the investigated catalysts. It should be noted, however, that apart from CO₂/H₂ ratio (1/4), the experimental conditions (e.g. mass of catalyst, total flow rate, feed composition etc.) used in transient-MS experiments are not exactly the same with those used during catalytic performance tests under steady state conditions. For example, the gas hourly space velocity (GHSV) used

under steady state conditions was $56,000\text{ h}^{-1}$, whereas that used in transient-MS experiments was 8000 h^{-1} . It is well known that an improvement of CO_2 conversion at a given temperature is expected by decreasing space velocity, which may be responsible for the appearance of methane peak maximum at lower temperatures in the results presented in Fig. 4.

3.2.2. 5% Ru/TiO_2 catalysts

3.2.2.1. In situ FTIR spectra. Results of Fig. 1 and our previous study [16] showed that alkali addition over 5% Ru/TiO_2 catalysts does not affect significantly CO_2 methanation activity, the enhancement of which was found to be significantly lower compared to that obtained over alkali-promoted 0.5% Ru/TiO_2 catalysts. The main difference between physicochemical properties of 0.5 and 5% Ru/TiO_2 catalysts is the size of Ru crystallites (2.1 and 4.2 nm, respectively), which was found not to be varied upon alkali addition for both catalysts examined [16]. Taking into account that CO_2 methanation reaction is structure sensitive with respect to the metal, the observed behavior should be correlated with the effect of Ru crystallite size, which seems to be prevailed against to alkali promotion effect in the case of catalysts of large Ru particles.

In order to gain a better understanding on the effect of alkali addition on the surface of catalysts characterized by large Ru particles, in situ DRIFT experiments were performed over 5% Ru/TiO_2 and 5% $\text{Ru}/0.2\%\text{Na-TiO}_2$ catalysts under $1\%\text{CO}_2 + 4\%\text{H}_2$ (in He) flow. Results obtained from the unpromoted sample are shown in Fig. 5A. It is observed that the spectrum recorded at $25\text{ }^\circ\text{C}$ (trace a) is characterized by a single band at 2018 cm^{-1} assigned to CO species linearly-bonded on reduced Ru crystallites ($\text{Ru}_x\text{-CO}$) and several bands below 1700 cm^{-1} due to carbonate (1630, 1410 and 1248 cm^{-1}) and formate species (1576 and 1355 cm^{-1}) associated with TiO_2 support.

Increase of temperature at $200\text{ }^\circ\text{C}$ (trace d) under $1\%\text{CO}_2 + 4\%\text{H}_2$ flow results in a significant increase of the relative intensity of $\text{Ru}_x\text{-CO}$ band at the expense of bands due to formate/carbonate species,

indicating the transformation of the latter species to Ru-bonded carbonyls. A new weak band appears at 2061 cm^{-1} attributed to multi-carbonyl species adsorbed on partially oxidized Ru sites (Ru^{n+}), which disappears at temperatures higher than $250\text{ }^\circ\text{C}$. The spectra recorded above $250\text{ }^\circ\text{C}$ are dominated by the band attributed to $\text{Ru}_x\text{-CO}$, which red-shifts to 1993 cm^{-1} at $450\text{ }^\circ\text{C}$ (trace i).

As discussed above, the formation of Ru^{n+} sites can be formed either by the oxidative disruption of small Ru clusters with the participation of hydroxyl groups of the support and/or by dissociative adsorption of CO on reduced Ru sites. The former explanation seems more reasonable for the 5% Ru/TiO_2 catalyst, since, as in the case of the unpromoted 0.5% Ru/TiO_2 catalyst, no evidence for the occurrence of the Boudouard reaction has been provided in the spectra shown in Fig. 5A. The significantly lower intensity of the band due to $\text{Ru}^{n+}(\text{CO})_x$ species (2061 cm^{-1}) (Fig. 5A), compared to that recorded for the catalyst of lower Ru loading (Fig. 2A), has been previously attributed to a decrease of the length of metal/support interface with increasing Ru particles [9]. This decrease results in suppression of the interaction of ruthenium atoms with the hydroxyl groups of TiO_2 support, and consequently, in elimination of partially oxidized Ru sites.

The lower metal/support interface may also responsible for the absence of the band attributable to $(\text{TiO}_2)\text{Ru-CO}$ species on the surface of 5% Ru/TiO_2 catalyst. It should be noted, however, that the latter band may exist, but its relative intensity may be too low and superimposed by the $\text{Ru}_x\text{-CO}$ band. Interestingly, the relative intensity of the $\text{Ru}_x\text{-CO}$ band (ca. 2015 cm^{-1} , trace c of Fig. 5A) is significantly higher over the 5% Ru/TiO_2 catalyst compared to 0.5% Ru/TiO_2 catalyst (ca. 2020 cm^{-1} , trace c of Fig. 2A), which exhibits significantly lower catalytic activity (Fig. 1A). This supports our previous suggestions that CO species linearly bonded on reduced Ru crystallites are potential methane precursors.

In Fig. 5B are shown the in situ DRIFT spectra obtained from the 5% $\text{Ru}/0.2\%\text{Na-TiO}_2$ catalyst following interaction with a flowing $1\%\text{CO}_2 + 4\%\text{H}_2$ (in He) mixture in the temperature range of $25\text{--}450\text{ }^\circ\text{C}$.

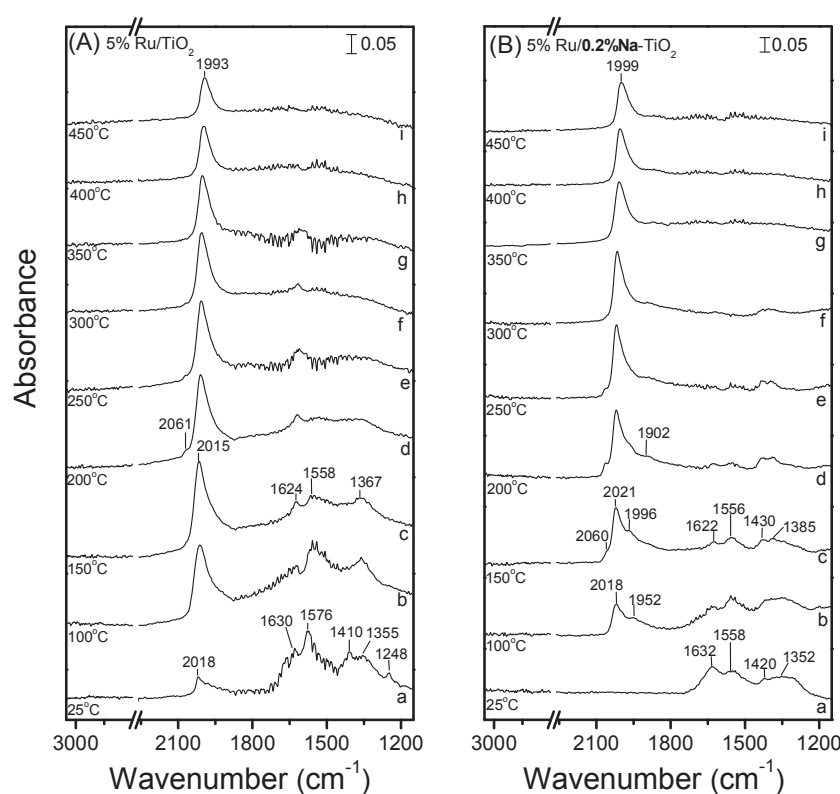


Fig. 5. DRIFT spectra obtained over (A) 5% Ru/TiO_2 and (B) 5% $\text{Ru}/0.2\%\text{Na-TiO}_2$ catalysts following interaction with $1\%\text{CO}_2 + 4\%\text{H}_2$ (in He) at $25\text{ }^\circ\text{C}$ for 15 min and subsequent stepwise heating at $450\text{ }^\circ\text{C}$ under the same flow.

The main difference observed compared to the spectra obtained from the unpromoted 5%Ru/TiO₂ (Fig. 5A), is the appearance of a band at 1952 cm⁻¹ at 100 °C (trace b), which is assigned to (TiO₂)Ru-CO species. This provides additional evidence that the number of sites located at the metal/support interface increases upon alkali addition.

Comparison of the results presented in Fig. 5B with those obtained from 0.5%Ru/0.2%Na-TiO₂ (Fig. 2C) catalyst shows significant differences in the nature and relative population of adsorbed CO species at temperatures lower than ca 350 °C. The main difference is related to the absence of the band attributable to Ruⁿ⁺-CO, as well as the significantly lower intensity of band due to Ruⁿ⁺(CO)_x. This indicates that when sodium is added on Ru/TiO₂ catalysts of large Ru particles, the catalyst is able to convert CO₂ into adsorbed CO species, but the latter cannot be dissociated into Ru-C and Ru-O in such amounts that would enable the formation of partially oxidized Ru sites and the detection of Ruⁿ⁺(CO)_x and Ruⁿ⁺-CO bands in the DRIFTS spectra of Fig. 5B. This is also supported by the absence of bands due to CH_{x,ads} species, indicating that the formation of surface carbon species is not operable on the surface of Na-promoted 5%Ru/TiO₂ catalysts. It could be assumed that the reaction rate of 5%Ru/0.2%Na-TiO₂ catalyst is too high and therefore, the formation of Ruⁿ⁺(CO)_x, Ruⁿ⁺-CO and CH_{x,ads} species takes place fast, making difficult their detection in the spectra of Fig. 5B. However, this could not be the case for the results of the present study since the specific activity of 5%Ru/0.2%Na-TiO₂ catalyst is only slightly higher than that of 0.5%Ru/0.2%Na-TiO₂ (Fig. 1A), where the above species are clearly discernible. In addition, although the band assigned to (TiO₂)Ru-CO species was detected on the surface of 5%Ru/0.2%Na-TiO₂ catalyst, its relative intensity is significantly lower compared to Ru_x-CO band in the entire temperature range examined. The opposite was observed for all Na-promoted 0.5%Ru/TiO₂ catalysts at temperatures lower than 150 °C (Fig. 2) and could be explained taking into account that, in general, the perimeter of the metal/support interface decreases with increasing Ru crystallite size.

Based on our previous studies, CO₂ hydrogenation reaction is structure sensitive, i.e., catalytic activity of Ru/TiO₂ increases by two orders of magnitude with increasing ruthenium crystallite size in the range of 0.9–4.2 nm [9,27]. Thus, it can be suggested that the effect of Ru crystallite size on catalytic activity predominates compared to the effect of alkali promotion over large Ru crystallites. Therefore, large Ru particles do not “feel” the presence of the promoter and CO₂ methanation activity cannot be further improved.

4. Conclusions

The nature of active sites and the CO₂ hydrogenation pathway have been investigated over 0.5%Ru/TiO₂ catalysts promoted with alkali metals, which have been previously shown to improve both catalytic activity and selectivity for the CO₂ methanation reaction. Results showed that hydrogenation of CO₂ proceeds with intermediate formation of carbonyl species via the RWGS reaction, the nature and population of which vary significantly in the presence of alkalis. Alkali addition results in an increase of the relative population of monocarbonyl species adsorbed on reduced Ru sites, which may be responsible for the improved CO₂ methanation activity. The detection of carbonyl species adsorbed on partially oxidized Ru sites, followed by CO₂ evolution in the gas phase and formation of CH_{x,ads} species on the surface of alkali-promoted 0.5%Ru/TiO₂ catalysts, provide evidences that CO dissociation and hydrogenation of surface carbon is favored upon promotion of well dispersed Ru catalysts with alkalis. The addition of sodium on 5%Ru/TiO₂ catalyst does not significantly affect neither the CO₂ methanation activity nor the nature and population of surface species formed under reaction conditions. Taking into account our previous findings that CO₂ methanation reaction is structure sensitive, i.e., TOF increases with increasing mean Ru crystallite size, it is suggested that the beneficial effect of sodium is suppressed with increasing Ru crystallite size, most possibly due to the predominance of the influence of Ru particle

size on the CO₂ methanation activity.

Acknowledgements

The author gratefully acknowledges the support of the Laboratory of Heterogeneous Catalysis of the Department of Chemical Engineering of the University of Patras in providing time on FTIR spectrometer.

Appendix A. Supplementary data

Supplementary material related to this article can be found, in the online version, at doi:<https://doi.org/10.1016/j.apcatb.2018.05.028>.

References

- [1] D. Heyl, U. Rodemerck, U. Bentrup, *ACS Catal.* 6 (2016) 6275–6284.
- [2] A. Karelovic, P. Ruiz, *Appl. Catal. B: Environ.* 113–114 (2012) 237–249.
- [3] M. Jacquemin, A. Beuls, P. Ruiz, *Catal. Today* 157 (2010) 462–466.
- [4] W. Li, X. Nie, X. Jiang, A. Zhang, F. Ding, M. Liu, Z. Liu, X. Guo, C. Song, *Appl. Catal. B: Environ.* 220 (2017) 397–408.
- [5] J.A.H. Dreyer, P. Li, L. Zhang, G.K. Beh, R. Zhang, P.H.L. Sit, W.Y. Teoh, *Appl. Catal. B: Environ.* 219 (2017) 715–726.
- [6] P. Frontera, A. Macario, M. Ferraro, P. Antonucci, *Catal. Today* 7 (2017) 59.
- [7] X. Su, J. Xu, B. Liang, H. Duan, B. Hou, Y. Huang, *J. Energy Chemistry* 25 (2016) 553–565.
- [8] W. Wei, G. Jinlong, *Front. Chem. Sci. Eng.* 5 (2011) 2–10.
- [9] P. Panagiotopoulou, *Appl. Catal. A: Gen.* 542 (2017) 63–70.
- [10] Q. Pan, J. Peng, T. Sun, S. Wang, S. Wang, *Catal. Commun.* 45 (2014) 74–78.
- [11] S. Rönsch, J. Schneider, S. Matthischke, M. Schlüter, M. Götz, J. Lefebvre, P. Prabhakaran, S. Bajohr, *Fuel* 166 (2016) 276–296.
- [12] J.H. Kwak, L. Kovarik, J. Szanyi, *ACS Catal.* 3 (2013) 2449–2455.
- [13] T.K. Campbell, J.L. Falconer, *Appl. Catal.* 50 (1989) 189–197.
- [14] X. Hu, G. Lu, *Green Chem.* 11 (2009) 724–732.
- [15] M.C. Bacariza, R. Bértolo, I. Graça, J.M. Lopes, C. Henriques, *J. CO₂ Util.* 21 (2017) 280–291.
- [16] A. Petala, P. Panagiotopoulou, *Appl. Catal. B: Environ.* 224 (2018) 919–927.
- [17] F. Solymosi, I. Tombácz, J. Kosztolay, *J. Catal.* 95 (1985) 578–586.
- [18] M. Guo, G. Lu, *RSC Adv.* 4 (2014) 58171–58177.
- [19] L. Xu, H. Yang, M. Chen, F. Wang, D. Nie, L. Qi, X. Lian, H. Chen, M. Wu, *J. CO₂ Util.* 21 (2017) 200–210.
- [20] Z.L. Zhang, A. Kladi, X.E. Verykios, *J. Catal.* 148 (1994) 737–747.
- [21] A. Beuls, C. Swalus, M. Jacquemin, G. Heyen, A. Karelovic, P. Ruiz, *Appl. Catal. B: Environ.* 113 (2012) 2–10.
- [22] E. Baraj, S. Vagaský, T. Hlinčík, K. Ciahotný, V. Tekáč, *Chem. Pap.* 70 (2016) 395–403.
- [23] I.A. Fisher, A.T. Bell, *J. Catal.* 162 (1996) 54–65.
- [24] G.D. Weatherbee, C.H. Bartholomew, *J. Catal.* 87 (1984) 352–362.
- [25] M. Marwood, R. Doepper, A. Renken, *Appl. Catal. A: Gen.* 151 (1997) 223–246.
- [26] P. Panagiotopoulou, D.I. Kondarides, X.E. Verykios, *Catal. Today* 181 (2012) 138–147.
- [27] P. Panagiotopoulou, X.E. Verykios, *J. Phys. Chem. C* 121 (2017) 5058–5068.
- [28] F. Solymosi, A. Erdöhelyi, T. Bánsági, *J. Catal.* 68 (1981) 371–382.
- [29] X. Wang, Y. Hong, H. Shi, J. Szanyi, *J. Catal.* 343 (2016) 185–195.
- [30] X. Wang, H. Shi, J.H. Kwak, J. Szanyi, *ACS Catal.* 5 (2015) 6337–6349.
- [31] F. Wang, S. He, H. Chen, B. Wang, L. Zheng, M. Wei, D.G. Evans, X. Duan, *J. Am. Chem. Soc.* 138 (2016) 6298–6305.
- [32] J. Xu, X. Su, H. Duan, B. Hou, Q. Lin, X. Liu, X. Pan, G. Pei, H. Geng, Y. Huang, T. Zhang, *J. Catal.* 333 (2016) 227–237.
- [33] M. Gratzel, J. Kiwi, K.R. Thampi, Mixed ruthenium catalyst, Google Patents, 1989.
- [34] F. Solymosi, A. Erdöhelyi, M. Kocsis, *J. Chem. Soc. Faraday Trans. Phys. Chem. Condensed Phases* 77 (1981) 1003–1012.
- [35] N. Kruse, J. Schweicher, A. Bundhoo, A. Frennet, T. Visart de Bocarmé, *Top. Catal.* 48 (2008) 145–152.
- [36] P. Panagiotopoulou, D.I. Kondarides, X.E. Verykios, *J. Phys. Chem. C* 115 (2011) 1220–1230.
- [37] B.H. Sakakini, *J. Mol. Catal. A Chem.* 127 (1997) 203–209.
- [38] J.W.A. Sachtler, J.M. Kool, V. Ponec, *J. Catal.* 56 (1979) 284–286.
- [39] A. Karelovic, P. Ruiz, *J. Catal.* 301 (2013) 141–153.
- [40] L.F. Liao, C.F. Lien, D.L. Shieh, M.T. Chen, J.L. Lin, *J. Phys. Chem. B* 106 (2002) 11240–11245.
- [41] L. Mino, G. Spoto, A.M. Ferrari, *J. Phys. Chem. C* 118 (2014) 25016–25026.
- [42] C. Elmasides, D.I. Kondarides, W. Grünert, X.E. Verykios, *J. Phys. Chem. B* 103 (1999) 5227–5239.
- [43] F. Solymosi, J. Raskó, *J. Catal.* 115 (1989) 107–119.
- [44] C. Elmasides, D.I. Kondarides, S.G. Neophytides, X.E. Verykios, *J. Catal.* 198 (2001) 195–207.
- [45] O.S. Alexeev, S.Y. Chin, M.H. Engelhard, L. Ortiz-Soto, M.D. Amiridis, *J. Phys. Chem. B* 109 (2005) 23430–23443.
- [46] Y.H. Kim, E.D. Park, H.C. Lee, D. Lee, *Appl. Catal. A: Gen.* 366 (2009) 363–369.
- [47] C.S. Kellner, A.T. Bell, *J. Catal.* 71 (1981) 296–307.
- [48] N.M. Gupta, V.S. Kamble, R.M. Iyer, K.R. Thampi, M. Gratzel, *J. Catal.* 137 (1992)

473–486.

- [49] G.H. Yokomizo, C. Louis, A.T. Bell, *J. Catal.* 120 (1989) 15–21.
- [50] J.L. Robbins, *J. Catal.* 115 (1989) 120–131.
- [51] S. Eckle, Y. Denkowitz, R.J. Behm, *J. Catal.* 269 (2010) 255–268.
- [52] F.M. Hoffmann, M.D. Weisel, J. Paul, *Surf. Sci.* 316 (1994) 277–293.
- [53] H.J. Freund, M.W. Roberts, *Surf. Sci. Rep.* 25 (1996) 225–273.
- [54] P. Panagiotopoulou, D.I. Kondarides, *J. Catal.* 260 (2008) 141–149.
- [55] P. Panagiotopoulou, D.I. Kondarides, *J. Catal.* 267 (2009) 57–66.
- [56] J.H. Pazmiño, M. Shekhar, W. Damion Williams, M. Cem Akatay, J.T. Miller, W. Nicholas Delgass, F.H. Ribeiro, *J. Catal.* 286 (2012) 279–286.
- [57] D.C. Grenoble, M.M. Estadt, D.F. Ollis, *J. Catal.* 67 (1981) 90–102.
- [58] J. Benziger, R.J. Madix, *Surf. Sci.* 94 (1980) 119–153.
- [59] M.P. Kiskinova, *Surf. Sci.* 111 (1981) 584–594.
- [60] D. Tománek, K.H. Bennemann, *Surf. Sci.* 127 (1983) L111–L117.
- [61] J. Onsgaard, S.V. Hoffmann, P.J. Godowski, P. Moller, J.B. Wagner, A. Groso, A. Baraldi, G. Comelli, G. Paolucci, *Chem. Phys. Lett.* 322 (2000) 247–254.
- [62] H. Wise, J.G. McCarty, *Surf. Sci.* 133 (1983) 311–320.
- [63] E.I. Kauppi, R.K. Kaila, J.A. Linnekoski, A.O.I. Krause, M.K. Veringa Niemelä, *Int. J. Hydrogen Energy* 35 (2010) 7759–7767.